Eur. Phys. J. B **14**, 73–82 (2000)

THE EUROPEAN PHYSICAL JOURNAL B
EDP Sciences

Localization effects in the charge density wave state of the quasi-two-dimensional monophosphate tungsten bronzes $(PO_2)_4(WO_3)_{2m}$ $(m = 7, 8, 9)$

J. Dumas[1,a], C. Hess[1], C. Schlenker[1], G. Bonfait[2,3], E. Gomez Marin[2], D. Groult[4], and J. Marcus[1]

[1] Laboratoire d'Études des Propriétés Électroniques des Solides[b], BP 166, 38042 Grenoble Cedex 9, France
[2] Departamento de Quimica, ITN, 2686 Sacavem Codex, Portugal
[3] Faculdade de Ciencias e Tecnologia, Universidade Nova de Lisboa, 2825 Monte de Caparica, Portugal
[4] Laboratoire CRISMAT[c], ISMRA, Université de Caen, 14050 Caen Cedex, France

Received 16 September 1999

Abstract. The monophosphate tungsten bronzes $(PO_2)_4(WO_3)_{2m}$ are quasi-two-dimensional conductors which show charge density wave type electronic instabilities. We report electrical resistivity and magnetoresistance measurements down to 0.30 K and in magnetic fields up to 16 T for the $m = 7, 8$ and 9 members of this family. We show that these compounds exhibit at low temperature an upturn of resistivity and field dependences of the magnetoresistance characteristic of localization effects. We discuss the dimensionality of the regime of localization as m is varied. We show that for $m = 7$, the regime is quasi-two-dimensional and three-dimensional for $m = 8, 9$.

PACS. 71.45.Lr Charge-density-wave systems – 72.15.Gd Galvanomagnetic and other magnetotransport effects

1 Introduction

Quasi low dimensional conductors are known to exhibit two types of electronic instabilities, either a Peierls type one towards a charge density wave (CDW) state or a superconducting one. In the transition metal bronzes $A_xM_yO_z$ where A is a cation or any group of elements inducing a partial filling of the conduction band, the CDW instability seems to be the dominant mechanism. The existence of Peierls transitions is associated to Fermi surfaces (FS) showing so-called nesting properties in the normal high temperature state. These instabilities give rise either to metal-semiconductor transitions, as it is the case in the quasi-1D molybdenum blue bronzes, if the FS is completely destroyed by the gap openings, or to metal-metal transitions if electron and hole pockets are left on the Fermi surface. This is the case of the quasi-2D molybdenum purple bronzes $A_{0.9}Mo_6O_{17}$ (A= K, Na) and of the monophosphate tungsten bronzes with the general formula $(PO_2)_4(WO_3)_{2m}$ where m is an integer which can be varied from 4 to 14 [1–5].

These latter series of compounds have been synthetized and their crystal structure studied more than a decade ago [6]. Their lattice is orthorhombic or monoclinic (pseudo-orthorhombic) and built with perovskite ReO_3-type infinite layers of WO_6 octahedra parallel to the a b plane, separated by PO_4 tetrahedra. Since the $5d$ conduction electrons are located in the perovskite $[WO_3]$-type slabs, the electronic properties are quasi-2D and the FS in the normal state is quasi-cylindrical. The thickness of the perovskite $[WO_3]$-type slabs and therefore the c parameter, are increasing with m, while a and b are only weakly dependent on it. The number of electrons per primitive cell is always 4 and independent of m while the average number of conduction electrons per W atom is $2/m$. The lower carrier density is therefore decreasing with m which may lead to a weaker screening and to an increase of electron-electron interactions. These compounds show high Peierls temperatures, above room temperature for large values of m [4].

The $m = 7$ member shows two successive Peierls transitions at $T_{p1} = 188$ K and $T_{p2} = 60$ K [7]. Both transitions are associated with the existence of several harmonics of the incommensurate CDW satellite wavevectors [8]. The second transition at T_{p2} is detected by X-ray studies only. In this $m = 7$ member a superconducting transition takes place at temperatures close to 0.30 K. This compound is, at present, the only known superconductor in the series of monophosphate tungsten bronzes and in the family of the quasi-2D oxide bronzes [9].

In the $m = 8$ member, two incommensurate CDW modulations are detected but no long range order is

[a] e-mail: dumas@lepes.polycnrs-gre.fr
[b] CNRS
[c] CNRS UMR 6508

achieved by cooling down to the lowest measurement temperature of ~ 35 K. Only a short range order can be observed. In the $m = 9$ member, two commensurate CDW modulations towards a long range order occur. The existence of higher order harmonics of the CDW satellites show that the instabilities are not conventional Peierls transitions [10].

In this article, we report electrical resistivity and magnetoresistance measurements down to 0.30 K and in magnetic fields up to 16 T for the $m = 7, 8$ and 9 members. Some preliminary results are given in reference [11]. We show that these compounds all exhibit at low temperature an increase of resistivity characteristic of quantum interference effects. The dimensionality of the regime of localization when m is varied is discussed and intrinsic or extrinsic mechanisms which may be involved are proposed for the different values of m.

2 Experiment and results

Single crystals used in these studies have been grown from mixtures of $(NH_4)_2HPO_4$ and WO_3 as starting materials by chemical vapor transport technique [12,13]. The crystals are platelets parallel to the (a, b) conducting plane and have typical size ($2 \times 0.5 \times 0.05$ mm^3). In order to obtain low contact resistance, the samples were washed firstly in acetone and secondly in a 20% HF bath for one hour; rapidly after this washing, silver pads of 500 Å were evaporated: contact resistance typically less than 10 Ω was obtained. Due to the anisotropic transport properties of these compounds, special care was taken in order to optimize the homogeneity of the current lines: the silver pads were evaporated to cover also the edge of the samples. With this method, unnested voltage [14] less than 10% the measured voltage was easily obtained. The thermopower was measured using a slow ac technique [15] between 4.2 K and 300 K. The resistivity was obtained by standard four point ac or dc technique and usually measured up to 6 T and between 4.2 K and 300 K (600 K for $m = 8$ and $m = 9$ samples). Some of the best samples have been measured up to 16 T and down to 0.3 K. In most of the magnetoresistance measurements the magnetic field was applied perpendicularly to the a, b plane with electrical current flowing in this highly conducting plane. The results reported here are obtained on samples for which the Peierls transitions have been detected both by transport measurements and X-ray diffraction studies. Since it is well-known that CDWs are easily destroyed by defects, the samples used in this study are expected to be of high quality.

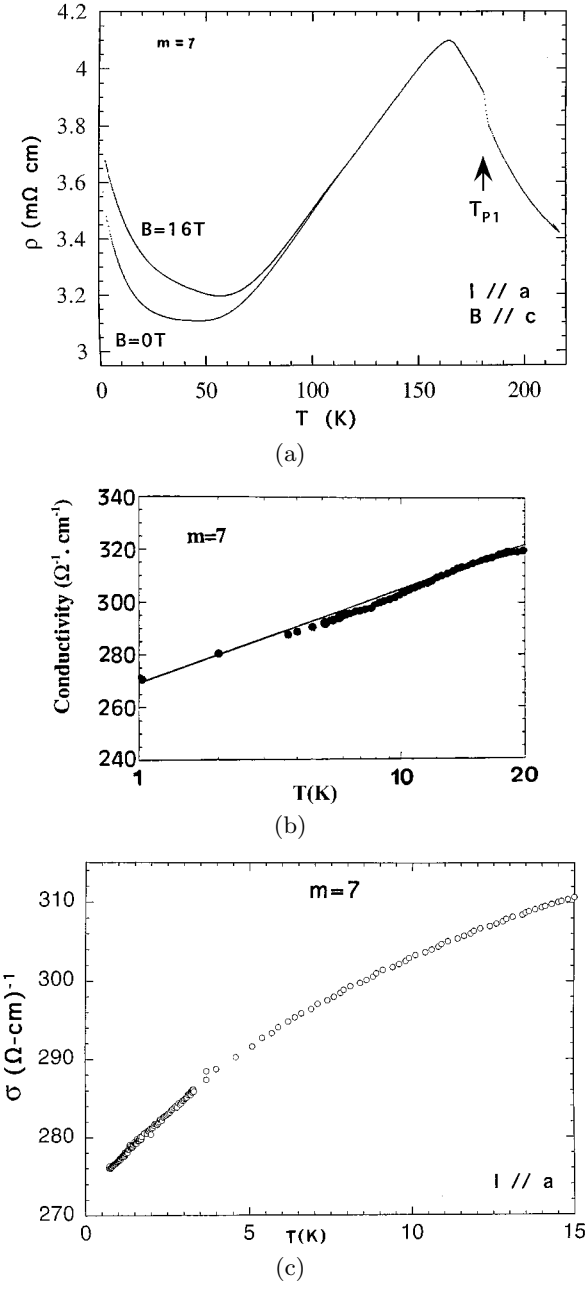

Fig. 1. (a) Resistivity and magnetoresistivity of a $m = 7$ sample; current I along the crystallographic a direction and magnetic field parallel to c. (b) Conductivity *vs.* logarithm of temperature for $T < 20$ K, ($m = 7$). (c) Conductivity *vs.* temperature for $T < 15$ K; current along the a direction; ($m = 7$).

2.1 m = 7 compound

Below room temperature, on decreasing the temperature, the resistivity (Fig. 1a) increases up to 170 K where an abrupt change occurs, associated to the first Peierls transition ($T_{p1} = 188$ K). Below this temperature, the resistivity still increases, reaches a rather sharp maximum (~ 165 K) and decreases down to a broad minimum without signature of the second Peierls transition ($T_{p2} = 60$ K). The $\rho(T)$ curve shows thermal hysteresis between roughly 100 K and T_{p1} [15].

Below ~ 20 K, the conductivity obeys a $\ln T$ law (Fig. 1b). Linear or square root temperature dependences may also give a good fit to the data but are valid in a much more restricted temperature interval (Fig. 1c). At $T = 0.3$ K, this compound enters a superconducting phase

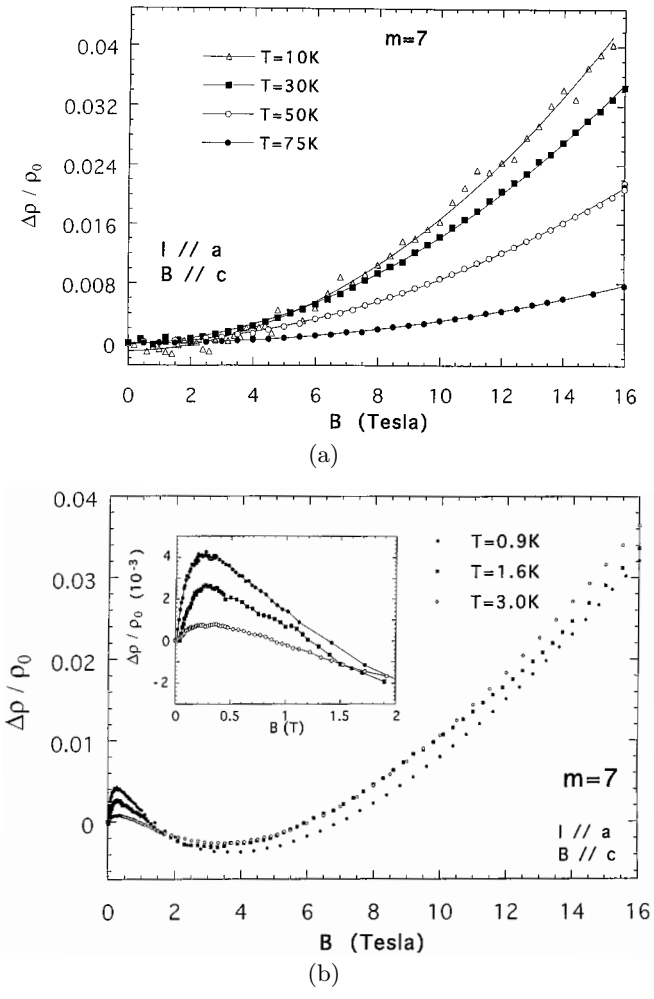

Fig. 2. (a) Magnetoresistance of a $m = 7$ sample as a function of magnetic field, at indicated temperatures. (b) Magnetoresistance of a $m = 7$ sample as a function of magnetic field at low temperatures ($T < 3$ K); current along the crystallographic a direction and magnetic field along c. The insert shows the low field part of the magnetoresistance.

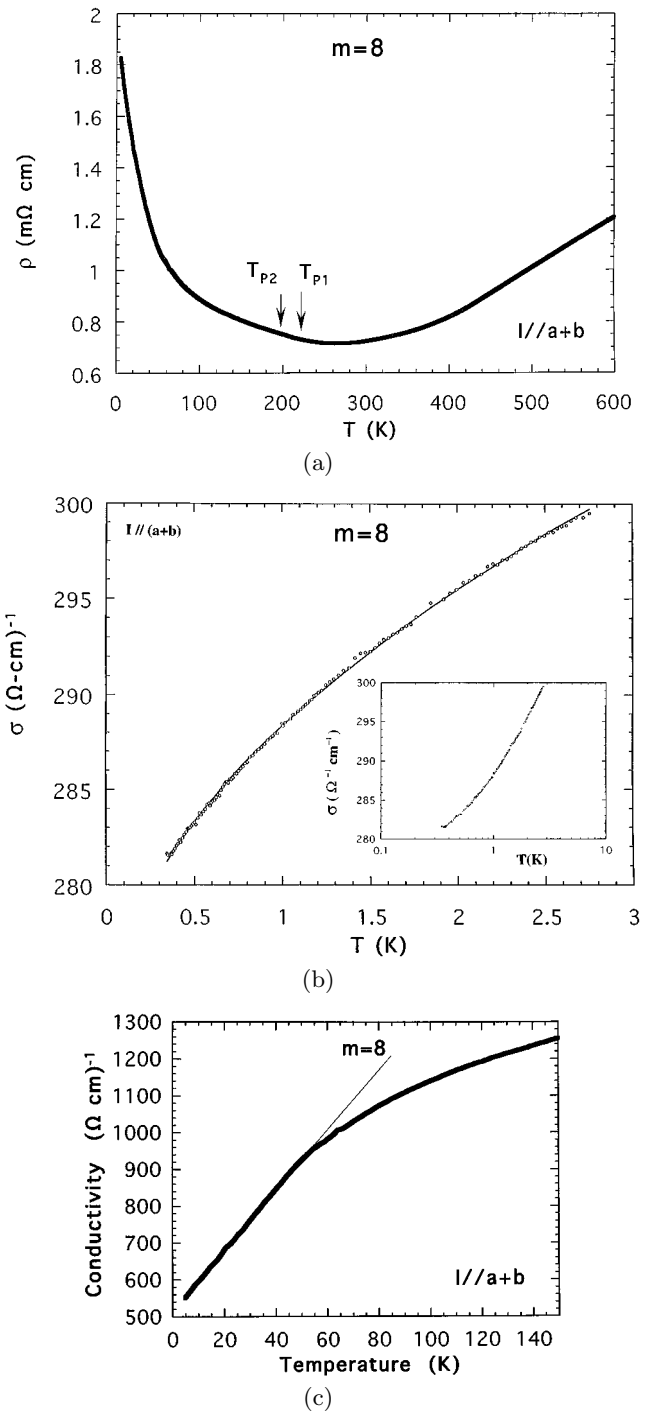

Fig. 3. (a) Resistivity *vs.* temperature for a $m = 8$ sample; current along $(a+b)$ axis. (b) Conductivity *vs.* temperature at $T < 3$ K for a $m = 8$ sample; current along $(a + b)$ axis. Solid line is a fit according to a $T^{1/2}$ law. Insert: conductivity *vs.* logarithm of temperature. (c) Conductivity *vs.* temperature at $T < 140$ K for a $m = 8$ sample; current along $(a + b)$ axis.

described elsewhere [9]. In Figure 1a is also shown a resistivity curve obtained with a magnetic field of 16 T applied parallel to the c axis. The resistivity behaviour is not strongly modified by the magnetic field, the main difference being a more pronounced resistivity minimum shifted to higher temperature (~ 60 K). Let us note that T_{p2} is not associated with an onset of the magnetoresistance as it has been observed for the Peierls transitions of the low m compounds [4]. For $T > 10$ K, the magnetoresistance (MR) increases quadratically with magnetic field (Fig. 2a). For lower temperatures (Fig. 2b), the MR is more complex: it first increases up to $B \sim 0.3$ T then decreases, becomes negative and passes through a large minimum before it reaches a quadratic regime similar to that obtained at high temperature. This non-monotonous low field behaviour is reminiscent of what occurs in some disordered systems [16].

2.2 m = 8 compound

The resistivity of the $m = 8$ compound was measured between 0.3 K and 600 K (Fig. 3a). At high temperature

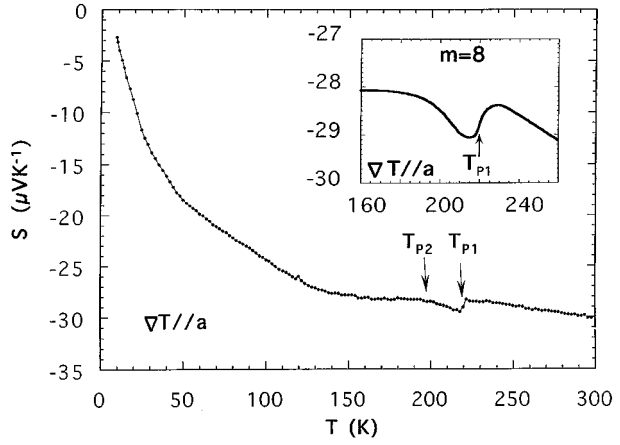

Fig. 4. Thermoelectric power *vs.* temperature for a $m = 8$ sample; thermal gradient along the crystallographic a direction. The insert shows the anomaly near $T_{\rm p1}$.

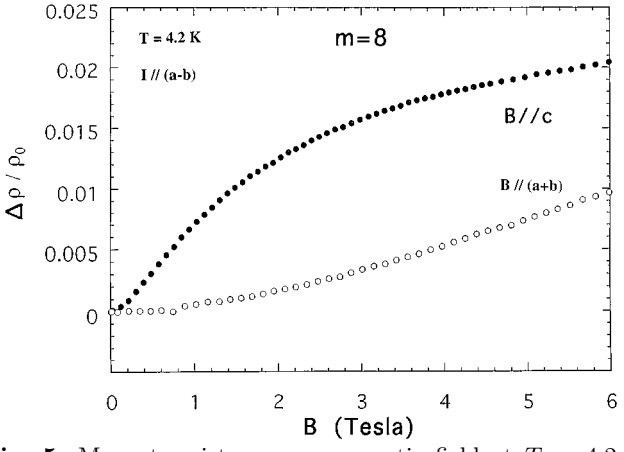

Fig. 5. Magnetoresistance *vs.* magnetic field at $T = 4.2$ K for two orientations of the magnetic field $B \parallel c$, $B \parallel (a + b)$; current along $(a - b)$ direction.

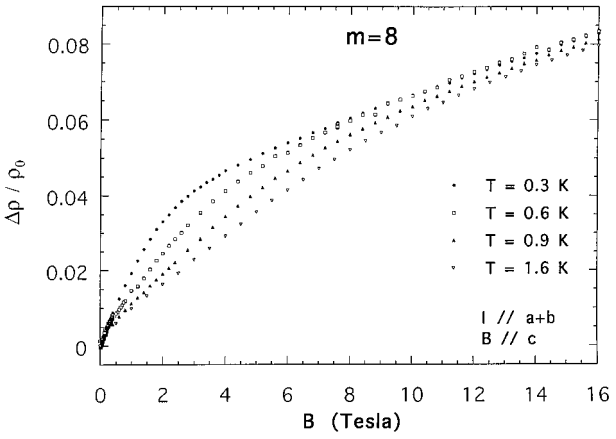

Fig. 6. Magnetoresistance *vs.* magnetic field at $T < 1.6$ K for a $m = 8$ sample; $B \parallel c$; $I \parallel (a + b)$.

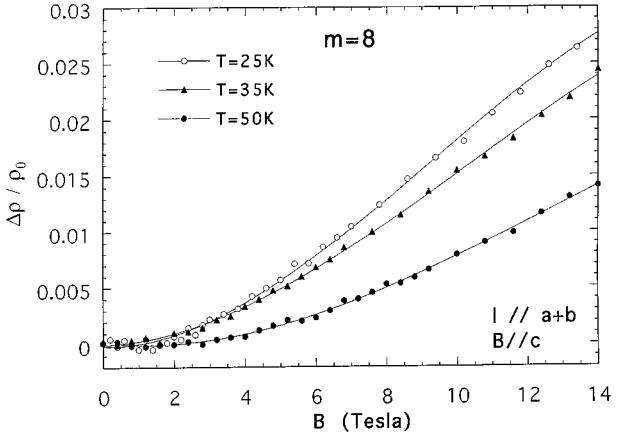

Fig. 7. Magnetoresistance *vs.* magnetic field at indicated temperatures; $B \parallel c$; $I \parallel (a + b)$.

($T > 300$ K), the resistivity is metallic type ($\mathrm{d}\rho/\mathrm{d}T > 0$). A broad minimum occurs just below room temperature and for some samples a weak change in the slope can be detected at the Peierls transitions ($T_{\rm p1} \sim 220$ K, $T_{\rm p2} \sim 200$ K). The increase of the resistivity on lowering temperature becomes faster below 50 K. For $T < 3$ K, the conductivity is well-described by a square-root law (Fig. 3b). Between ~ 5 K and 50 K, the conductivity increases approximately linearly with T (Fig. 3c). In contrast with the $m = 7$ compound, the $\ln T$ behaviour for the conductivity is not observed, as illustrated in the insert of Figure 3b.

The thermopower (TEP) is always negative and its absolute value increases with increasing temperature in the range 8 K–300 K (Fig. 4). A TEP anomaly (inset Fig. 4) between 170 K and 230 K signals the two Peierls transitions detected by X-ray diffraction. The value of the TEP is similar to that of the low m compounds.

The MR of the $m = 8$ compound is positive and anisotropic on the whole explored range of temperature and magnetic field. However, as in the $m = 7$ compound, two temperature ranges for the MR must be considered. Below 10 K (Fig. 5), the MR varies rapidly for fields up to 0.5 T and slows down at higher field. The MR is larger for B parallel to the c^* direction than for B parallel to the (a, b) plane.

Let us note that at very low temperature (~ 0.3 K), the MR displays a hump around 3 T which disappears progressively at higher temperature (Fig. 6). For $T > 10$ K, a quadratic regime is reached similar to that obtained in the $m = 7$ compound (Fig. 7).

2.3 m = 9 compound

The resistivity of the $m = 9$ compound was measured between 0.3 K and 600 K (Fig. 8a). The resistivity coefficient $\mathrm{d}\rho/\mathrm{d}T$ is always negative down to 200 K and the Peierls transitions ($T_{\rm p1} = 565$ K, $T_{\rm p2} = 330$ K) as obtained by X-ray diffuse scattering [10] are not clearly identified on the $\rho(T)$ curve. Below 50 K, similarly to the $m = 7$ and $m = 8$ compounds, the resistivity increases with decreasing temperature. No sign of superconductivity was detected down to 0.3 K. Below ~ 40 K, the conductivity increases approximately linearly with temperature (Fig. 8b). The MR

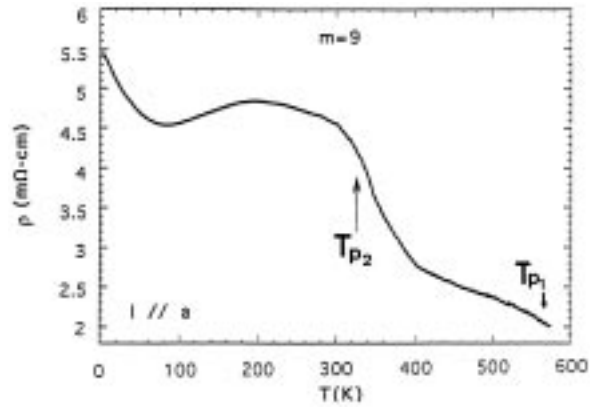

(a)

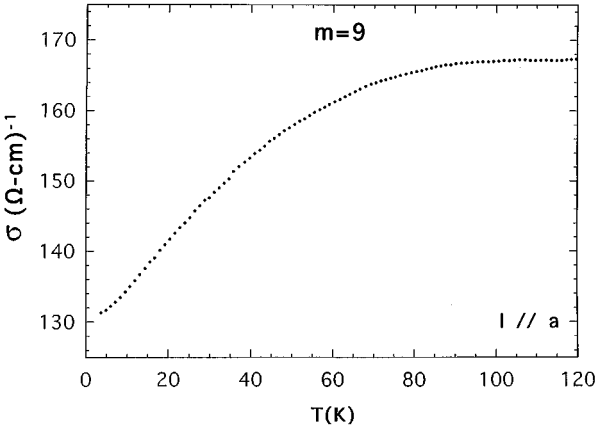

(b)

Fig. 8. (a) Resistivity as a function of temperature for a $m = 9$ sample; current along the a direction. (b) Conductivity as a function of temperature, $m = 9$ sample; current along a.

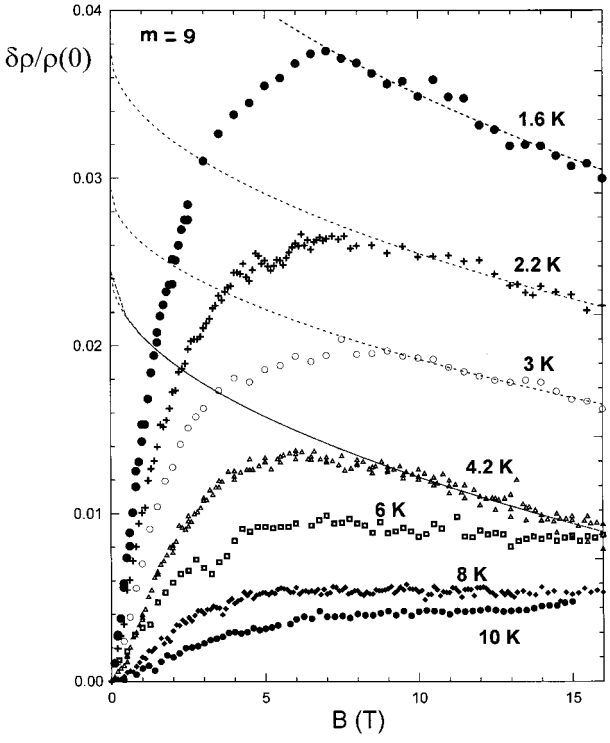

(a)

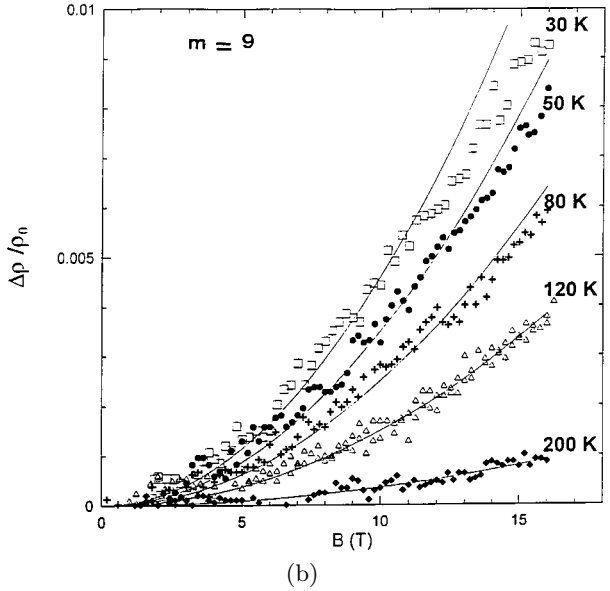

(b)

Fig. 9. (a) Magnetoresistance as a function of magnetic field for a $m = 9$ sample at $T < 10$ K. Dotted lines are fit according to equation (8). (b) Magnetoresistance as a function of magnetic field for a $m = 9$ sample at $T > 30$ K. Solid lines are fit according to a quadratic law.

behaves similarly to that of the $m = 7$ compound: at low T, the MR increases linearly with magnetic field (Fig. 9a) up to 7 T and slowly decreases at higher fields. The field corresponding to the maximum of the MR (~ 7 T) is approximately temperature independent and is found to be much higher than that found for the $m = 7$ compound (0.3 T). At higher temperature (Fig. 9b), the B^2 regime is recovered as in the other compounds, with a B^2 coefficient smaller than that of the $m = 7$ compound. In the whole range of field and temperature explored, the MR is always positive, in contrast with the complex MR behaviour observed in the $m = 7$ compound where a negative MR is found at very low temperatures.

Let us now summarize the main experimental results on the $m = 7, 8, 9$ compounds and compare them to that obtained on the $m = 4, 5, 6$ ones. At low temperature ($T < 50$ K), the resistivity coefficient $\mathrm{d}\rho/\mathrm{d}T$ of the "high-m compound" is always negative contrarily to "the low-m compounds" family, in which the resistivity behaviour at low T is similar to that of a metal with a residual resistivity less than 1 mΩ cm. For the "high-m compounds", the resistivity at low temperatures is larger than 1 mΩ cm. The MR at low T does not show any Shubnikov-de Haas oscillations as observed in the $m = 4, 5, 6$ compounds [17] and is comparatively small: for instance, at 4.2 K and 6 T, $\Delta\rho/\rho$ is always less than 3% whereas for the low m-family, in the same conditions, $\Delta\rho/\rho$ is of order of 100%. Clearly, the basic interpretation of these transport measurements at low T need a more elaborated model than that of nearly

free electrons used for the low-m compounds. In the next part of this article, it will be shown that quantum interference effects may satisfactorily account for these results.

3 Discussion

3.1 Peierls transition and CDW state

The Peierls instability in the $m = 7$ compound appears as an anomaly on the resistivity *vs.* temperature curve. Above T_{p1}, the increase of ρ on lowering the temperature could be due to the existence of a pseudogap. This has been suggested earlier with respect to pretransitional streaks on the X-ray patterns [8]. The observed increase of ρ below T_{p1} is a general feature of Peierls transitions and is attributed to a loss of carriers as the partial Peierls gap opens. At lower temperatures, the CDW state of $m = 7$ is characterized by a metallic behaviour of the resistivity associated with the remaining parts of the Fermi surface. The strong thermal hysteresis, which has also been observed on the intensity of CDW satellite reflections [8], is not understood at the moment. It could be due to metastable configurations of CDW. A second CDW transition has been observed by X-ray studies at $T_{p2} = 60$ K [8]. It could be related to the change of slope of ρ *vs.* T at low temperatures but does not appear as a distinct anomaly as it is the case for T_{p1}. One may note that both charge density wave anomalies in this compound are associated with non-sinusoidal modulations of the satellite wavevectors and therefore with unconventional CDW states.

The $m = 8$ compound shows two successive Peierls instabilities. Unlike all other compounds of the series, the associated CDW-wavevectors of both transitions do not condense into distinct satellite spots even at the lowest temperatures as revealed by X-ray diffuse scattering studies [10]. This implies that the CDWs are correlated over a finite distance only. The high temperature metallic behaviour of the resistivity can be attributed to the undistorted Fermi surface in the normal state. The minimum and the increase of ρ at lower temperatures might be due to the gradual opening of Peierls gaps at T_{p1} and T_{p2}. However, one also has to consider the possibility of an intrinsic disorder caused by the uncorrelated CDWs which could decrease the conductivity. The minimum of ρ at 260 K and the very weak anomalies at T_{p1} and T_{p2} could be a hint to a pseudogap regime above the Peierls transitions, similarly to the one suggested for $m = 7$. The thermoelectric power shows distinct anomalies at the transition temperatures, which reflects a modification of the Fermi surface by the CDW gap openings. The negative sign of the thermoelectric power indicates that the majority charge carriers are electrons in both the CDW and normal state of $m = 8$.

Resistivity *vs.* temperature data on $m = 9$ do not show a distinct anomaly at T_{p1}. One should note that the slope $d\rho/dT$ is negative in the normal and CDW state as well as in the $m = 9$ as in the $m = 7$ compound. Below T_{p1}, the maximum of the resistivity could be due to the gradual opening of the Peierls gap, affecting the Fermi surface and the charge carriers.

3.2 Low temperature regime

3.2.1 Theoretical background

a) Weak localization

All three compounds discussed here show an increase of the resistivity at low temperatures upon cooling. We observed temperature and magnetic field variations of the resistivity that can be interpreted in the framework of weak localisation theory [16,18,19].

In the case of weak disorder, the elastic mean free path of an electron in a lattice is very short when compared with the inelastic one. The motion of conduction electrons, moving between two points in a crystal lattice is diffusive. It is characterized by an electron diffusion constant D which is related to the electrical conductivity σ and the density of states at the Fermi level $n(\varepsilon_F)$ by the Einstein relation:

$$D = \sigma/e^2 n(\varepsilon_F). \quad (1)$$

Among the various paths an electron can travel between two points of the lattice, there is the particular case of the electron returning to its starting point. In this case, the partial wavefunctions of the electron along this path can interfere constructively and the quantum mechanical probability of the returning path is enhanced by a factor of two compared with the classical probability. Such processes lead to weak localization and are responsible for an increase of the resistivity.

The constructive interference of the partial electron wavefunctions can be destroyed by the effect of a magnetic field B and inelastic scattering with electrons or phonons. The corresponding scattering time for inelastic scattering τ_{ie} is :

$$\tau_{ie}^{-1} = \tau_{ee}^{-1} + \tau_{ep}^{-1} \quad (2)$$

where τ_{ee} is the electron-electron and τ_{ep} the electron-phonon scattering time. They have characteristic temperature dependences following power laws T^{-p} with $1.5 < p < 2$ and $2 < p < 4$ for electron-electron [20] and electron-phonon scattering [21] respectively.

An electromagnetic vector potential causes a phase shift of the partial electron wavefunctions and thus destroys their phase-coherence. This is known as the Aharonov-Bohm effect. It is associated with a magnetic scattering time $\tau_B = \hbar/4eDB$. Finally, let us consider the spin-orbit scattering time, τ_{so}, which is related to the interaction of the spin of the conduction electron with the orbital momentum. This effect is responsible for a reduction of the return probability of the electron.

The quantum correction to the conductivity is, in the three dimensional (3D) case [22]:

$$\delta\sigma \sim \frac{e^2}{\hbar L_\varphi} + \text{const.} \quad (3)$$

$L_\varphi = (D\tau_\varphi)^{1/2}$ is the phase coherence length, with $\tau_\varphi \sim T^{-p}$.

In the two-dimensional (2D) case,

$$\delta\sigma_{\rm d} \sim \frac{-e^2}{\hbar} \ln L_\varphi/\ell \tag{4}$$

where ℓ is the mean free path and $\sigma_{\rm d} = \sigma_a$ where a is the transverse size of the system.

An expression for the magnetoresistance has been given by Altshuler and Aronov in the 3D case [19,23]:

$$\frac{\Delta\rho(B)}{\rho} = -\rho\frac{e^2}{2\pi^2\hbar}\sqrt{\frac{eB}{\hbar}}\left[f_3\left(\frac{4DeB\tau_\varphi}{\hbar}\right)\right] \tag{5}$$

where f_3 is the Kawabata function [24] with limiting values:

$$f_3(x) = \begin{cases} 0.605 & x \gg 1 \\ x^{3/2}/48 & x \ll 1 \end{cases}. \tag{6}$$

For strong magnetic fields ($x \gg 1$) the magnetoresistance decreases and follows the law:

$$\frac{\Delta\rho(B)}{\rho} = -0.605\rho\frac{e^2}{2\pi^2\hbar}\sqrt{\frac{eB}{\hbar}}\,.$$

In the 2D case [23], for B perpendicular to the plane of the system,

$$\frac{\Delta\rho(B)}{\rho} = -\rho\frac{e^2}{2\pi^2\hbar} f_2\left(\frac{4DeB\tau_\varphi}{\hbar}\right) \tag{7}$$

with

$$f_2(x) = \begin{cases} \ln x & x \gg 1 \\ x^2/24 & x \ll 1 \end{cases}.$$

b) Electron-electron interaction effects

In the presence of strong elastic scattering, the conduction electrons can also interact with each other. Unlike the preceding case where interactions are neglected, we consider now two interacting electrons with energies near the Fermi level having a difference of the order of $k_{\rm B}T$. The phase coherence of their wavefunctions is destroyed after a time $\tau_{\rm T} \approx \hbar/k_{\rm B}T$. An expression for the correction to the conductivity in the 3D case due to electron-electron interaction (EEI) has been derived [25]:

$$\delta\sigma \propto \sqrt{\frac{k_{\rm B}T}{\hbar D}}\,. \tag{8}$$

In the 2D case, the correction can be written [25]:

$$\delta\sigma \propto \sqrt{\frac{k_{\rm B}T}{\hbar D}} \times \frac{\ln T\tau}{\hbar}\,. \tag{8'}$$

The magnetoresistance arising from spin splitting of conduction electron energies has been calculated by Lee and Ramakrishnan [26]:

$$\frac{\Delta\rho(B)}{\rho} = \rho\frac{e^2}{2\pi^2\hbar}\,\frac{\tilde{F}_\sigma}{2}\sqrt{\frac{k_{\rm B}T}{2\hbar D}}\, g_3\left(\frac{g^*\mu_{\rm B}B}{k_{\rm B}T}\right) \tag{9}$$

where the function $g_3(x)$ for the 3D case has the limiting values $\sqrt{x} - 1.3$ for $x \gg 1$ and $0.053x^2$ for $x \ll 1$. g^* is the effective Landé factor of the electron. $\tilde{F}_\sigma$ is a function which depends on the screening constant in a Hartree-Fock approach.

In the 2D case, $\frac{\Delta\rho}{\rho} \propto g_2(x)$.

The function $g_2(x)$ has the limiting behaviours: with

$$g_2(x) = \begin{cases} \ln(x/1.3) & x \gg 1 \\ 0.084x^2 & x \ll 1 \end{cases} \tag{10}$$

3.2.2 Analysis

a) m = 7 compounds

We can evaluate the diffusion constant in the case of the $m = 7$ compound by equation (1) with values from the electrical conductivity and from the linear contribution γT to the specific heat at low temperatures. With the γ value obtained in reference [15a], ($\gamma = 136 \pm 14$ mJ mole^{-1}K^{-2}) and with $\gamma = \pi^2 k_{\rm B}^2 n(\varepsilon_{\rm F})/3$, one obtains $D = 5.4 \times 10^{-2}$ cm^{2}s^{-1} as determined from the extrapolated conductivity at $T = 0$ K. This low diffusivity value is comparable to what is found in a number of disordered transition metal oxides (*i.e.*; in the class of ABO_3 compounds) showing weak localization effects [27].

At very low temperatures, the $\ln T$ behaviour of the conductivity is consistent with equation (4) with $\tau_\varphi \sim T^{-p}$. It is characteristic of a quasi-2D regime, valid for weak localization effects and electron-electron interactions. This law is not observed in the $m > 7$ compounds.

We attribute to a classical contribution the high field behaviour of the magnetoresistance, which follows a B^2 law up to high temperatures. In an earlier paper [7], we have evaluated the number of carriers and their mobilities by using a fairly simple two-band model (one band hole- and one band electron-like) associated with spherical Fermi surfaces. Mobilites in the range of 140 cm^{2}V^{-1}s^{-1} had been obtained at $T = 4.2$ K. These values are much smaller than those found in the compounds with low m values ($m = 4, 6$) [4]. This result together with negative magnetoresistance effects corroborate our weak localization approach.

b) m = 8 compound

The results obtained on the $m = 8$ compound can also be interpreted in the framework of quantum interference effects. The diffusion constant can be obtained from the conductivity and specific heat data. The linear coefficient of the specific heat has been found to be $\gamma = 14$ mJ mole^{-1}K^{-1} [15b]. The diffusion constant is then $D = 3.5 \times 10^{-1}$ cm^{2}s^{-1}. This value is well above that of the $m = 7$ compound.

The thermal dependence of the electrical conductivity (Figs. 3a, b) reveal two regimes of quantum interference effects. The $T^{1/2}$ behaviour for $T < 3$ K is characteristic of a 3D regime of electron-electron interactions while the linear regime below ~ 40 K is characteristic of a 3D

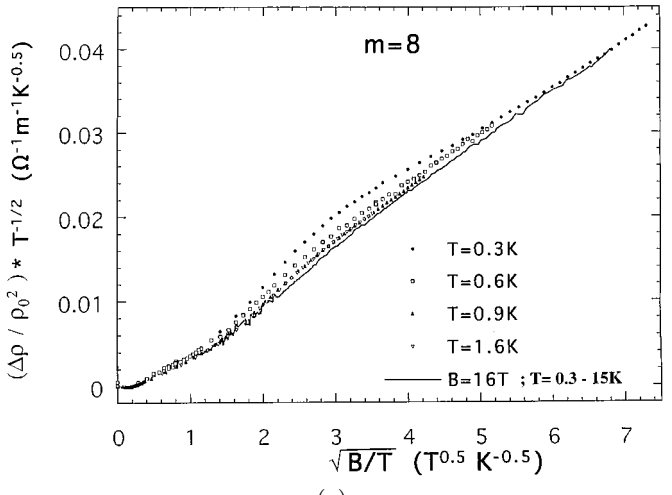

(a)

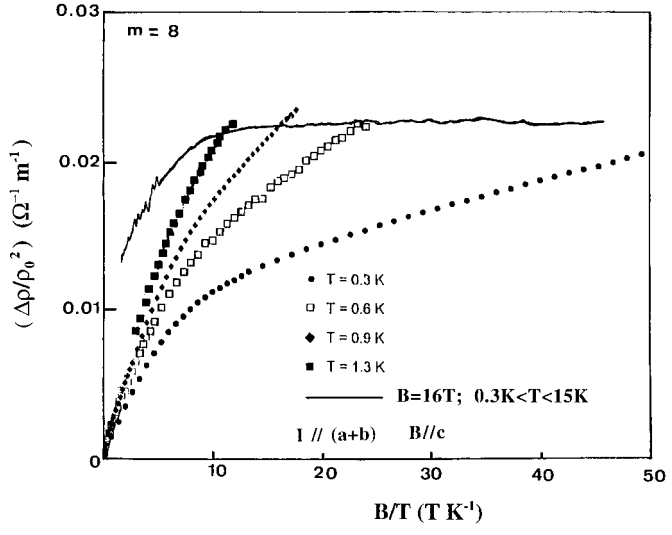

(b)

Fig. 10. (a) $(\Delta\rho/\rho^2)T^{-1/2}$ as a function of $(B/T)^{1/2}$ for a $m = 8$ sample (see text). Dots correspond to the same data as in Figure 6; solid line: data obtained at fixed field $B = 16$ T as a function of temperature. (b) $(\Delta\rho/\rho^2)$ as a function of B/T for a $m = 8$ sample (see text).

regime of weak localization which could be associated to the presence of fluctuating CDW domains.

Contrarily to the $m = 7$ compounds, the magnetoresistance of the $m = 8$ compound is always positive and increases monotonically up to 16 T and down to 0.3 K. This behaviour can be explained by a consequence of electron-electron interactions. The magnetoresistance due to these interactions is given in the 3D case by a scaling law of the form:

$$\frac{\Delta\rho(B)}{\rho^2\sqrt{T}} = \alpha\sqrt{\frac{B}{T}} - \beta \qquad (11)$$

which corresponds to equation (9) in the limit $x \gg 1$. Figure 10a shows a plot of $\frac{\Delta\rho(B)}{\rho^2\sqrt{T}}$ *versus* $\sqrt{\frac{B}{T}}$ for the experimental data with the magnetoresistance obtained as a function of magnetic field at fixed temperatures (dots) and as a function of temperature at fixed field values (line). Except for $T = 0.3$ K, all curves superimpose. The above scaling law (Eq. (11)) is well-obeyed except for $T = 0.3$ K. In the limit of small $\sqrt{B/T}$ values, the plot shows a positive curvature as expected from the limit of $g_3(x)$ for $x \ll 1$.The plot becomes linear for higher values of $\sqrt{B/T}$ as expected from $g_3(x)$ for $x \gg 1$.

Table 1. Comparison of the coefficients α, β obtained from the fit of the magnetoresistance data to the electron-electron interactions model; $m = 8$ compound.

$m = 8$	experimental	theoretical
$\alpha\ \left(\Omega^{-1}\mathrm{cm}^{-1}\mathrm{T}^{-1/2}\right)$	5.5	5.4
$\beta\ \left(\Omega^{-1}\mathrm{cm}^{-1}\mathrm{K}^{-1/2}\right)$	2.3	2.2

The obtained coefficients α and β are in good agreement with the theoretical values (Tab. 1). At lower $\sqrt{B/T}$ values, Figure 10a shows a hump related with the low temperature data. This hump disappears at higher temperatures. It is possibly due to a classical origin or to a contribution of weak localization. Figure 10b shows a plot of the experimental data using the 2D model. The curves do not superimpose. A 3D model for the quantum interference effects is therefore appropriate.

For $T > 4.2$ K, the magnetoresistance shows a quasi-linear dependence with the magnetic field. Although a B^2 is predicted by (Eq. (9)), the experimental values are too large to be accounted for. This behaviour has therefore probably a classical origin.

c) m = 9 compound

The quasi linear temperature dependence of the conductivity below $\sim$ 40 K is characteristic of a 3D regime of weak localization. At magnetic fields such that $\frac{g\mu_B B}{k_B T} \gg 1$, the magnetoresistance decreases with increasing B and follow a $B^{1/2}$ law (Fig. 9a):

$$\Delta\rho/\rho = -\eta B^{1/2}.$$

We can then deduce the coefficient η from this fit and compare it to the theoretical value given in equation (6) in the limit $x \gg 1$. We find $\eta = 5 \times 10^{-3}\ \Omega\mathrm{mT}^{-1/2}$, of the same order of magnitude as the theoretical value $7.2 \times 10^{-3}\ \Omega\mathrm{mT}^{-1/2}$.

3.2.3 Possible sources of disorder

The presence of quantum interference effects is due to an elastic mean free path short compared to the inelastic one. This comparatively short elastic mean free path is due to disorder. One should therefore analyse the possible sources of disorder in the monophosphate tungsten bronzes $(PO_2)_4(WO_3)_{2m}$ with $m > 6$. Electron microscopy studies show clearly that stacking faults of WO_3

layers corresponding to different m values are more and more frequent when m is increased [28]. This corresponds to intergrowth of layers of different m values compounds. This kind of planar defects cannot be eliminated and have to be taken into account in the large m phases. Since it is unlikely that the impurities concentration is larger in large m compounds than in the small m ones, we suggest that the localization effects are generally due to these intergrowth defects.

In the special case of the $m = 8$ compound, the CDW do not develop long range order down to the lowest temperatures. One therefore cannot exclude that these local uncorrelated Peierls lattice distortions may have an effect on the transport properties and represent a possible source of intrinsic disorder besides the mechanisms mentioned above. This disorder might be temperature dependent and related to the size of the fluctuating CDW domains.

3.2.4 Dimensionality

The variation of the dimensionality observed in the localisation properties is striking. Our results indicate a crossover between a 2D regime and a 3D one between the compounds $m = 7$ and $m = 8$ and 9. The interlayer coupling is expected to decrease when m is increased, which would increase the low dimensionality character. One should note that the thickness of the WO_3 layers increases regularly with the c axis parameter when m is increased. However, the c-axis parameter increases only by $\sim 20\%$ when m varies from 7 to 9 [29]. Therefore, we suggest that the change of dimensionality between the $m = 7$ and $m = 8$ and 9 is rather due to a rapid decrease of L_φ with increasing m. When L_φ becomes smaller than the layer thickness, a three-dimensional behaviour is expected to be dominant. The decrease of L_φ may be related to an increase of disorder from $m = 7$ to $m = 8$ and 9, probably induced by a larger number of intergrowth defects. This latter mechanism is an additional one to the effect of the increase of the layer thickness with m. Anyhow, these results indicate that the transverse coupling does not play a major role for the localization properties and that the transport data are dominated by the intralayers processes.

4 Conclusion

In summary, electrical resistivity and magnetoresistance measurements have provided information on the low temperature CDW state of the $(PO_2)_4(WO_3)_{2m}$ phosphate tungsten bronzes for $m = 7, 8, 9$. All compounds exhibit an upturn of resistivity at low temperatures. We have shown that quantum interference effects can explain the resistivity and magnetoresistance data at low temperatures. These properties may be due to disorder induced by the intergrowth of layers corresponding to different m values in the large m compounds, since such properties are not observed in low m ($m < 7$) compounds.

The dimensionality of the regime of localization is found to vary with m. For $m = 7$, a quasi-two dimensional description is appropriate. This latter compound is a system which allows further studies of the interplay between charge density wave, superconductivity and localization effects. For the $m = 8$ and $m = 9$ compounds, three-dimensional models of quantum interference effects can describe satisfactorily the results. The change of dimensionality between the $m = 7$ and $m = 8$ and 9 compounds may be due to a rapid decrease of L_φ associated to an increase of disorder when m is increased.

This work was supported in part by the program Human Capital and Mobility of the European Union under Contract ERBCHRXCT940616. C. Hess is grateful for a fellowship from the Land Baden-Württemberg, Germany.

References

1. *Low Dimensional Electronic Properties of Molybdenum Bronzes and Oxides*, edited by C. Schlenker (Kluwer Acad. Pub., 1989).
2. M. Greenblatt Ed., Int. J. Mod. Phys. B **7**, 4045 (1993).
3. C. Schlenker, J. Dumas, M. Greenblatt, S. van Smaalen, *Physics and Chemistry of Low Dimensional Inorganic Conductors, NATO ASI Series B*, vol. **354** (Plenum, 1996).
4. C. Schlenker, C. Hess, C. Le Touze, J. Dumas, J. Phys. I France **6**, 2061 (1996).
5. C. Hess, C. Schlenker, J. Dumas, M. Greenblatt, Z.S. Teweldemedhin, Phys. Rev. B **54**, 4581 (1996).
6. Ph. Labbé, M. Goreaud, B. Raveau, J. Solid State Chem. **61**, 324 (1986); M. Borel, M. Goreaud, A. Grandin, Ph. Labbé, A. Leclaire, B. Raveau, J. Sol. Inorg. Chem. **28**, 93 (1991).
7. A. Rötger, C. Schlenker, J. Dumas, Synth. Metals **55–57**, 2670 (1993); A. Rötger, Thesis, Université Joseph Fourier, Grenoble, 1993 (unpublished); A. Rötger, J. Lehman, C. Schlenker, J. Dumas, J. Marcus, Z.S. Teweldemedhin, M. Greenblatt, Europhys. Lett. **25**, 23 (1994).
8. P. Foury, J.P. Pouget, Int. J. Mod. Phys. B, **7** (23 & 24), 3973 (1993).
9. C. Hess, C. Schlenker, G. Bonfait *et al.*, Physica C **282–287**, 955 (1997); C. Hess, C. Schlenker, G. Bonfait *et al.*, Solid State Commun. **104**, 663 (1997).
10. A. Ottolenghi, J.P. Pouget, J. Phys. I France **6**, 1059 (1996).
11. C. Hess, C. Le Touze, C. Schlenker, J. Dumas, D. Groult, J. Marcus, Synth. Metals **86**, 2419 (1997); C. Hess, C. Schlenker, G. Bonfait, E. Gomez-Marin, D. Groult, J. Marcus, J. Dumas, Physica B **259–261**, 974 (1999).
12. Z.S. Teweldemedhin, K.V. Ramanujachary, M. Greenblatt, J. Solid State Chem. **95**, 21 (1991); Z.S. Teweldemedhin, K.V. Ramanujachary, M. Greenblatt, Phys. Rev B **46**, 7897 (1992).
13. J.P. Giroult, M. Goreaud, Ph. Labbé, B. Raveau, Acta Cryst. B **37**, 2139 (1981).
14. L.R. Bickford, K.K. Kanazawa, J. Solid State Chem. **37**, 839 (1976).

15. (a) J. Lehmann, C. Schlenker, C. Le Touze, A. Rötger, J. Dumas, J. Marcus, Z.S. Teweldemedhin, M. Greenblatt, J. Phys. IV France **3**, C2–243 (1993); (b) C. Hess, Thesis, Université Joseph Fourier, Grenoble, 1997 (unpublished), p. 198.
16. G. Bergmann, Phys. Rep. **107**, 1 (1984).
17. C. Le Touze, G. Bonfait, C. Schlenker, J. Dumas, M. Almeida, M. Greenblatt, Z.S. Teweldemedhin, J. Phys. I France **5**, 437 (1995).
18. E. Abrahams, P.W. Anderson, D.C. Licciardello, T.V. Ramakrishnan, Phys. Rev. Lett. **42**, 673 (1979).
19. B.L. Altshuler, A.G. Aronov, in *Electron-Electron Interaction in Disordered Systems, Modern Problems in Condensed Matter*, vol. 10, edited by A.L. Evros, M. Pollak, (North Holland Publ., 1985).
20. A. Schmid, Z. Phys. **271**, 251 (1974).
21. J. Rammer, A. Schmid, Phys. Rev. B **34**, 1352 (1986).
22. Reference [19], pp. 9–11.
23. Reference [19], pp. 108–109; B.L. Altshuler, A.G. Aronov, A.I. Larkin, D. Khmel'nitskii, JETP **54**, 411 (1981).
24. A. Kawabata, Solid State Commun. **34**, 431 (1980).
25. Reference [19], p. 81; B.L. Altshuler, A.G. Aronov, Solid State Commun. **46**, 429 (1983).
26. P.A. Lee, T.V. Ramakrishnan, Phys. Rev. B **26**, 4009 (1982).
27. M.A. Dubson, D.F. Holcomb, Phys. Rev. B **32**, 1955 (1985); A.K. Raychaudchari, Phys. Rev. B **44**, 8572 (1991); A.K. Raychaudhuri, Adv. Phys. **44**, 21 (1995).
28. B. Domengès (private communication, 1996); B. Domengès, P. Roussel, Ph. Labbé, D. Groult, J. Solid State Chem. **127**, 302 (1996).
29. B. Domengès, F. Struder, B. Raveau, Mat. Res. Bull. **18**, 872 (1983).